Testing models of ice cap extent, South Georgia, sub-Antarctic.

Barlow, N.L.M.[1,2*], Bentley, M.J.[1], Spada, G.[3], Evans, D.J.A.[1], Hansom, J.D.[4], Brader, M.D.[1], White, D.A.[5], Zander, A.[6], Berg, S.[7]

[1] Department of Geography, Durham University, South Road, Durham, DH1 3LE, UK

[2] School of Earth and Environment, University of Leeds, Leeds, LS2 9JT, UK

[3] Dipartimento di Scienze Pure e Applicate (DiSPeA) Urbino University ''Carlo Bo'', Urbino, Italy

[4] School of Geographical and Earth Sciences, University of Glasgow, Glasgow, G12 8QQ, UK

[5] Institute for Applied Ecology, University of Canberra, Canberra, ACT 2617, Australia.

[6] Institute of Geography, University of Cologne, Albertus-Magnus-Platz, 50923 Cologne, Germany

[7] Institute of Geology and Mineralogy, University of Cologne, Zülpicher Str. 49a, 50674 Cologne, Germany

* Corresponding author: n.l.m.barlow@leeds.ac.uk +44 113 343 3761

Keywords

Last Glacial Maximum, glacial isostatic adjustment, sea-level change, South Georgia, sub-Antarctic, coastal geomorphology

Abstract

The extent of Last Glacial Maximum ice in South Georgia is contested, with two alternative hypotheses: an extensive (maximum) model of ice reaching the edge of the continental shelf, or a restricted (minimum) model with ice constrained within the inner fjords. We present a new relative sea-level dataset for South Georgia, summarising published and new geomorphological evidence for the marine limit and elevations of former sea levels on the island. Using a glacial isostatic adjustment model (ALMA) specifically suited to regional modelling and working at high spatial resolutions, combined with a series of simulated ice-load histories, we use the relative sea-level data to test between the restricted and extensive ice extent scenarios. The model results suggest that there was most likely an extensive Last Glacial Maximum glaciation of South Georgia, implying that the island was covered by thick (>1000 m) ice, probably to the edge of the continental shelf, with deglaciation occurring relatively early (ca. 15 ka BP, though independent data suggest this may have been as early as 18 ka). The presence of an extensive ice cap extending to the shelf edge would imply that if there were any biological refugia around South Georgia, they must have been relatively localised and restricted to the outermost shelf.

Rationale and background

Though limited in size, the extent of glaciations of the sub-Antarctic islands, such as South Georgia, is of considerable interest due to their position in the Southern Ocean, providing a potential link between the climates of South America and West Antarctica (Hall, 2009; Hodgson et al., 2014a; 2014b). Moreover, the extent of ice has important implications as to whether the sub-Antarctic islands acted as glacial refugia for biota (Barnes et al., 2006; Barnes et al., 2016; Hodgson et al., 2014b; Hogg et al., 2011; Thatje et al., 2008). Though the contribution of the potential ice mass on South Georgia to global sea level will be modest, recent changes in glacier extent in response to 20th century warming (Cook et al., 2010; Gordon et al., 2008) demonstrates the sensitivity of maritime South Georgia to changes in climate and oceanographic forcing by the Southern Ocean. During the global Last Glacial Maximum (LGM), ice on South Georgia expanded (Bentley et al., 2007; Hodgson et al., 2014b; Sugden and Clapperton, 1977) but there remains significant debate about the maximum ice extent reached during this time. Two widely divergent models have been suggested for the size of the ice cap over South Georgia during the LGM: an extensive (maximum) model of ice reaching the edge of the continental shelf (during at least one glacial phase) (Sugden and Clapperton, 1977), or a restricted (minimum) model with ice being constrained within the inner fjords (Bentley et al., 2007). The aim of this paper is to use glacial-isostatic adjustment (GIA) modelling in association with geomorphological evidence of former marine limits and past sea levels, as a means to test between the alternative models of former ice cap extent on South Georgia.

The maximum model

The maximum model was suggested by Sugden and Clapperton (1977), based on the undulating and glacially scoured morphology of the continental shelf and the deep glacial troughs incised into it. They used precision depth recorder data to suggest that whereas the troughs are offshore extensions of fjords containing many features characteristic of glacier erosion, the areas between the troughs are characterised by irregular topography of the order of 20-80 m of relief. They argued

that these features are uncommon on 'normal' continental shelves where sediment deposition tends to obscure irregular relief. Based upon the limited offshore data available, they documented evidence for glacial areal scour almost everywhere on the shelf shallower than 200 m and estimate a maximum ice area of 30,000 km^2. Sugden and Clapperton (1977) suggested that this extensive shelf-extent glaciation must have predated the last island-wide glaciation of South Georgia based upon preserved beach material emplaced on land between two periods of glacial sedimentation.

New bathymetric data, including swath bathymetry of some key areas, led Graham et al. (2008) to suggest an extensive ice cap at the LGM but acknowledged that there was little dating evidence to support this. Their evidence included more detailed mapping of the troughs noted by Sugden and Clapperton (1977), as well as the discovery of submarine landforms interpreted as moraines, located in the troughs close to the shelf edge (Figure 1).

The minimum model

A minimum model for ice cap glaciation was suggested by Bentley et al. (2007) based on dated onshore geomorphological evidence mapped across a variety of fjords along the north-east coast of South Georgia. In particular, Bentley et al. (2007) mapped a consistent pattern of moraines that did not extend beyond the fjord mouths, and dated these using cosmogenic nuclide surface exposure dating. They also noted the low elevation (<10 m) of all post-glacial raised beaches, implying a minor amount of glacial isostatic rebound and a relatively small antecedent ice cap. Based on the geomorphology and cosmogenic exposure ages, and a well-dated lake sediment core implying ice-free inner fjords as early as 18,621–19,329 cal yr BP at the Tønsberg Peninsula (Rosqvist et al., 1999), Bentley et al. (2007) suggested that the ice did not extend beyond the fjord mouths at the LGM. Direct observations of recent behaviour of South Georgia glaciers has identified precipitation as the primary controlling factor on tidewater glaciers (Gordon and Timmis, 1992) and using this analogue

Bentley et al. (2007) suggested that the restricted extent of LGM glaciation may have been due to low precipitation caused by extensive sea ice presence upwind of South Georgia.

Hodgson et al. (2014a) used multibeam swath bathymetric surveys of nine major fjords around South Georgia to reveal a relatively consistent pattern of submarine geomorphological features. These include a shallow inner basin bounded by an inner basin moraine and a deep basin with a moraine at the outer limits of each of the fjords. Using a relative chronology based primarily on existing terrestrial evidence from Bentley et al. (2007), they suggested that the inner basin moraines date from the last major glacial advance (LGM), and the deep basin moraines from an earlier glaciation, possibly marine isotope stage (MIS) 6. However, they suggested offshore marine work is required to date the deglacial morainic sediments.

Timing of post-LGM deglaciation

Numerous studies have sought to date the timing of deglaciation on South Georgia using terrestrial proxies for ice retreat, of which Hodgson et al. (2014b) provide a comprehensive review. To date, the offshore evidence is limited to bathymetric surveys with little direct chronological control. The onshore oldest cosmogenic isotope dates mark the oldest mapped ice advance, estimated using an error-weighted mean to have been abandoned at 12.1 ± 1.4 yr BP (Bentley et al., 2007). The oldest evidence for post LGM ice-free conditions comes from the radiocarbon dates marking the onset of lake sedimentation in one basin on the Tønsberg Peninsula, close to Husvik, at 18,621–19,329 cal yr BP (Rosqvist et al., 1999). Most other basal dates from lake sediments and peat sequences provide minimum ages for ice-free conditions from the start of the Holocene (Table 1 in Hodgson et al., 2014b).

To test the two differing hypothesis of extensive (maximum) or restricted (minimum) ice limits during the LGM we develop two sets of ice models that simulate extensive (shelf based) or restricted

(island only) glaciation that we input into a GIA model, the outputs of which we compare to the geomorphological evidence of former relative sea levels (RSL) from the island. The results have implications for understanding of sub-Antarctic glaciation, ongoing patterns of land-level displacement and the climate of the Southern Ocean.

Study area

South Georgia is 170 km long and its width varies from 2 to 40 km (Figure 1). It is dominated by a central spine of mountains rising to nearly 3000 m (Mount Paget is the highest peak at 2935 m). The axis of the island hosts a series of linked icefields from which numerous outlet glaciers descend. Most terminate as tidewater fronts but a few have terrestrial margins. The glaciers have eroded deep fjords that dominate the South Georgia coastline and at the head of most of these is a large outlet glacier. South Georgia currently has a cool climate (mean annual temperature 2°C) with a strong maritime influence (Smith, 1960). The regional equilibrium line altitude (ELA) on the north-east of the island was estimated by Smith (1960) to be 460 m above sea level (asl). Much of the data reported here is focused on the north-east coast of the island where there are several ice-free peninsulas between the fjords which can be logistically accessed, and on which is located a rich geomorphological record of glacial landforms and raised coastal features (Bentley et al., 2007; Clapperton et al., 1989; Stone, 1974; Sugden and Clapperton, 1977). The south-west coast is data-poor since it is largely glaciated down to sea level, difficult to access, and has limited present and raised marine features (Hansom, 1979).

Field data

To test the hypothesis of extensive versus restricted ice extent during the LGM we compiled a dataset of geomorphological evidence of the elevation of past sea level (Figures 1, 2 and 3), to compare against the GIA model outputs. There is widespread and consistent evidence of the postglacial marine limit on South Georgia and a small number of dated sea-level index points.

146

147 *Raised marine features*

148 There is a wide range of raised marine features around the island, most of which have been
149 identified along the north-east coastline where previous work and our own mapping has focussed
150 (Figure 1, Tables 1 and 2). These can be divided into two main groups: raised beaches and rock
151 platforms. The raised beaches consist of an assemblage of common landforms that are always found
152 below 10 m asl, though are found above modern beach level either due to relative sea-level fall
153 and/or long-term tectonic uplift (Figures 1 and 2). They typically consist of raised gravel beaches and
154 terraces cut into existing glacial or slope deposits (e.g. Gordon and Hansom, 1986). The deposits are
155 usually crudely bedded gravels, small boulders and coarse sand, with subhorizontal layering. Most
156 of these are not directly dated. There are also a small number of landforms <10 m asl such as
157 isolation basins, and a dune complex that have allowed us to provide dated constraints on relative
158 sea-level change. We identify these low elevation features as post-LGM in age based on the
159 following characteristics: fresh appearance of sediments, lack of overlying glacial or slope sediments
160 and cross-cutting relationships with moraine deposits located in the fjords, as well as a small number
161 of direct ages on selected landforms (Table 1). We surveyed many of these beaches to add to the
162 raised gravel beaches surveyed by Stone (1974, 1976), and sequences of raised beaches at 2-4 m and
163 6-10 m noted by Hansom (1979) and Clapperton et al. (1989).

164

165 The second set of landforms consists of rock platforms, mostly located at present sea level and
166 between 20 and 50 m asl. These comprise prominent terraces backed by a cliff, usually cut into
167 bedrock, or occasionally surficial sediments, and are frequently consistent in elevation across sets of
168 adjacent headlands (Adie, 1964; Stone, 1974). The platforms have been discussed since Gregory
169 (1915) interpreted them as 'a wide plain of marine denudation', and have been reported as high as
170 150 m asl although few of the platforms >50 m have been unequivocally ascribed a marine origin
171 (Stone, 1974). The rock platforms around the island are usually capped by erratics and till and so

pre-date the last glaciation, especially as they extend under the most recent fjord and valley side moraines around the island (Bentley et al., 2007). For this reason we do not use them for directly constraining the GIA model output of post-glacial RSL change but they are useful for understanding the long-term landscape evolution of the island.

Clapperton (1971), Sugden and Clapperton (1977) and Clapperton et al. (1989) also noted the presence of older raised beaches at higher elevations than the post-LGM beaches. These are identified as older than post-LGM because they are partly lithified and cemented with iron oxide, and the well-rounded clasts of some are covered by, and incorporated into, till (Clapperton et al., 1989; Clapperton et al., 1978). They include examples in Kelp Bay (at 20m asl) and Harcourt Foreland the north side of Royal Bay (at 52m asl) (Sugden and Clapperton, 1977), and six other unnamed sites that occur up to 40 m asl along the south coast of the island (Clapperton et al., 1989). We therefore constrain the postglacial marine limit to be below 10 m asl with no evidence for post-LGM marine features above this elevation.

Dated constraints on relative sea-level change

Clapperton et al. (1978) showed that the highest beach they recorded in St Andrews Bay (6-7.2 m) was cut into a moraine and therefore formed after deglaciation from that moraine. Dates on the lowermost layer of peat accumulated on top of the till of the equivalent moraine in King Edward Cove yielded a radiocarbon age of 9493±370 ^{14}C yr BP (SRR-736), which thus provides a minimum age for the moraine. The beach was covered by a layer of peat which yielded a basal age of 3997±85 ^{14}C yr BP (SRR-597). Clapperton et al. (1978) therefore concluded that the highest beach was formed sometime between 9500 and 4000 ^{14}C yr BP (equivalent to a calibrated age between 9677–11832 and 4148-4645 cal yr BP). Calculating the indicative range of a raised marine beach is a challenge (Kelsey, 2015) and therefore we use the ages from Clapperton et al. (1978) in Figure 3 to constrain

197 the potential maximum and minimum ages for this feature, but apply a more conservative 6-10 m
198 range for the marine limit based upon the range of mapped elevations (Figure 1).
199
200 Stone (1979) reported a site on the south side of Royal Bay where a series of raised beaches at 6 m
201 asl extends into a sea-cave system. A fibrous mat of organic sediment including moulted seal skin
202 and hair yielded a radiocarbon age of 2369±40 ^{14}C yr BP (SRR-520). This provides a minimum age for
203 the 6m raised beach found at the back of the cave (Stone, 1979).
204
205 In Enten Valley the raised beaches are covered by a sequence of beach foredunes and shadow dunes
206 where at least seven large beach ridges (E1-7), and several smaller ridges are preserved across a 400
207 m wide strandplain (Figure 4 and supplementary information). Most of the inland dune sands are
208 indurated and covered by a thin (0.1-0.3 m) layer of peat, with soil and peat thicknesses generally
209 increasing inland, suggesting increasing age. Peat accumulations on the dunes are substantially
210 thinner than on the nearby (near sea level) moraines, which are commonly covered by over a metre
211 of peat, suggesting the beaches post-date the moraines by some time. New infrared stimulated
212 luminescence (IRSL) dating indicates that beach crests at 5 m above mean sea level were deposited
213 at or shortly before the 3810±350 a and 4350±400 a IRSL ages for the foredune basal sand that
214 overlies the top of the beach crest (further detailed in the supplementary information). Beach crests
215 at <2 m elevation are covered by dune sands and shadow dunes dated to 1180±110 a and 710±100 a
216 respectively. These ages imply that RSL fell from 4-5 m shortly after 4000 yr and has been below 1 m
217 since at least ~1200 yr.
218
219 Little Jason Lagoon is a coastal basin in inner Cumberland West Bay (54°11.568'S 36°35.469'W;
220 detailed in supplementary information). It is near-circular with a narrow entrance and shallow sill at
221 1 m (±0.5 m) depth. Analysis of a sediment core (Co1305) sampled from within the lagoon has
222 demonstrated that the sediments record a transition from freshwater (lacustrine) conditions to a

223 marine lagoon. The transition from a freshwater to marine environment has been identified on the
224 basis of $\delta^{13}C$ of TOC and diatom data with a commensurate increase in measured sulphur at the
225 point of isolation (Figure 5). Plant remains from 2 cm above the transition yield a radiocarbon age of
226 8966±106 ^{14}C yr BP (9662-10251 cal yr BP) giving a maximum age for the transition from freshwater
227 to marine conditions in the basin.

228

Site	**Elevation (m asl)**	**Material dated**	**^{14}C age (^{14}C yr BP)**	**Lab code**	**Age**	**Comment**	**Source**
King Edward Cove	7.2	Peat on moraine	9493±370	SRR-736	*9677-11832	Maximum age of 7.2 m beach	Clapperton et al. (1978)
Cumberland West Bay	7.2	Peat on raised beach	3997±85	SRR-597	*4148-4645	Minimum age of 7.2 m raised beach	Clapperton et al. (1978)
St Andrews Bay	6	Organic sediment including sea skin and hair	2369±40	SRR-520	*1369-1557	Minimum age for 6 m beach.	Stone (1979)
Little Jason Lagoon	-1 ± 0.5	Plant remains	8966±106		*9662-10251	Timing of freshwater-to-marine transition as RSL rose.	This study
Enten Bay	5.5	Sand		C-L3329	#3980±340	Minimum age for beach	This study
Enten Bay	5.5	Sand		C-L3330	#4350±100	Minimum age for beach	This study
Enten Bay	5.7	Sand		C-L3328	#3810±350	Minimum age for beach	This study
Enten Bay	1.5	Sand		C-L3332	#1180±110	Minimum age for beach	This study
Enten Bay	1.8	Sand		C-L3331	#710±100	Minimum age for beach	This study

229 **Table 1 -** Dated relative sea level constraints from South Georgia.

230 * (cal yr BP), radiocarbon ages calibrated using CALIB v.7.1 (http://calib.qub.ac.uk/) (Stuiver and
231 Reimer, 1993). Reported calibrated ages are the 2-sigma ranges, using the SH13 curve (Hogg et al.,
232 2013). Marine reservoir correction for seal hair taken as 750 yr (Sugden and John, 1973).
233 # IRSL ages (see Supplementary Info).
234
235 The dated RSL data points are compiled in Figure 3 to provide a series of constraints against which
236 the GIA model results can be compared, though the main constraint is the elevation of the ~6-10 m
237 marine limit.
238
239 **Glacial isostatic adjustment modelling**
240 Modelling of the solid earth response and resulting RSL changes to test the proposed maximum and
241 minimum ice scenarios is done using ALMA (Spada, 2008), which is specifically suitable for GIA
242 regional modelling and high spatial resolutions. ALMA implements the Post Widder formula and
243 computes the Love numbers for a spherical self-gravitating, layered, incompressible Earth model
244 with Maxwell rheology. The viscosity profile is a volume-average of the one adopted in Peltier's
245 (2004) Earth model VM2: lower mantle viscosity 2.7 x 10^{21} Pa s and upper mantle 0.5 x 10^{21} Pa s. The
246 lithosphere is elastic with a thickness of 90 km. There is no direct evidence for a low viscosity mantle
247 at this location and this allows us to integrate the ICE-5G (VM2) solutions computed in SELEN (Spada
248 et al., 2012; Spada and Stocchi, 2007) for far-field RSL changes driven by changes in the global ice
249 sheets from their LGM maximum (Figure 6). We do not use ICE-6G model (Argus et al., 2014; Peltier
250 et al., 2015) at this time due to uncertainties surrounding the Antarctic Peninsula component
251 (Purcell et al., 2016), which due to its proximity to South Georgia may have implication for our
252 results. Figure 6 shows that South Georgia experiences relatively minor far-field isostatic effects and
253 the resulting RSL signal from the global model is primarily due to changes in total ocean volume
254 (often termed the eustatic function) (Figure 6B). This global-model RSL curve is added to our local
255 predictions of RSL changes driven by our South Georgia ice-load models. It must be noted that the

256 ICE-5G (VM2) model of Peltier (2004) includes a compressible Earth structure, which may result in
257 ~0.1 mm yr^{-1} error when computed in our incompressible model.
258
259 Our modelling approach seeks to test the two different LGM hypotheses but does not aim to
260 accurately simulate the past ice cap topography due to the limited palaeo-glaciological constraints.
261 For this reason we use a simple 'slab' ice load in order to provide a simple but robust test between
262 extensive (whole continental shelf occupied by ice) and restricted (ice within the island coastline)
263 ice-load models. The extensive shelf model includes 2315 4.74 km diameter discs, with the
264 restricted island-only ice load comprising 202 discs (Figure 7). Using discs has been a long adopted
265 method for gridding ice load (e.g. Tushingham and Peltier, 1991) to minimise overlap and gaps. The
266 model is computed with 15,000 spherical harmonics to allow for the small load diameter (after Bevis
267 et al., 2016). Increasing the number of discs, i.e. decreasing their diameter, increases the
268 computational intensity at no benefit to the results (Bevis et al., 2016). We test different ice-model
269 thicknesses for each maximum and minimum ice scenario in order to understand the sensitivity of
270 our model output to local thickness changes. We develop 8 key scenarios which allow us to test the
271 maximum and minimum load hypotheses, applying ice loads at 1 k yr time-steps in different
272 combinations (Table 2), partly constrained by the geomorphological evidence discussed above. Ice-
273 load histories are given relative to present from 22 to 0 ka, with a constant load from 71 ka to the
274 LGM in order to allow reasonable equilibration of the ice load. In each of the extensive (shelf) or
275 restricted (island) ice models all the discs have the same stepwise ice-load history, and all ice models
276 include a 100 m thick load for the island-only discs at 4-3 ka and 1-0 ka to allow for Neoglacial and
277 recent ice advances (Bentley et al., 2007; Hall, 2009). The model does not allow for underlying
278 topographic variations and therefore the stated values are the uniform ice thickness, not the height
279 of the ice surface with respect to the underlying topography. The limited glaciological evidence for
280 the LGM ice-cap behaviour on South Georgia means that it is not currently feasible to develop

281 spatially variable time-retreating ice-load histories. The model outputs are computed for 12 key
282 locations (Figure 1) including four GPS stations (detailed in Table 3).
283

Model number	Description	Island (restricted) ice load	Shelf (extensive) ice load
1	Restricted, thin, island only load	22-12 ka: 100 m	-
2	Restricted, thick, island only load	22-12 ka: 1000 m	-
3	Restricted, very thick, island only load	22-21 ka: 3000 m 21-12 ka: 1000 m	-
4	Thick, LGM shelf load, post-LGM small, thin, island only load	22-21 ka: 1000 m 22-12 ka: 100 m	22-21 ka: 1000 m
5	Extensive, thin shelf load, until 15 ka	22-15 ka: 100 m	22-15 ka: 100 m
6	Extensive, thick shelf load, until 18 ka	22-18 ka: 1000 m	22-18 ka: 1000 m
7	Extensive, thick shelf load, until 15 ka	22-15 ka: 1000 m	22-15 ka: 1000 m
8	Extensive, thick shelf load, until 12 ka	22-12 ka: 1000 m	22-12 ka: 1000 m

Table 2 – South Georgia ice model scenarios used in ALMA

Results

The results of the ALMA RSL curves for the 12 observer locations on South Georgia, combined with the SELEN modelled ICE-5G RSL curve (Figure 6), are plotted in Figure 8 and compared with the RSL data and marine limit elevations. Fit with the data is assessed visually as the restricted number of available RSL data points and their marine limiting nature means a statistical assessment is not viable. Due to the simplicity of the ice model there is very little spatial variation between the 12 modelled observer locations during the Holocene, so the results are not plotted by separate colours in Figure 8 and are discussed for all the modelled South Georgia sites collectively. All the model outputs predict a rise from a post-LGM lowstand, with the pre-Holocene part of the RSL curves tracking the general RSL rise of the ICE-5G global modelled curve in Figure 6B.

The restricted ice-load models, which only contain ice on the island (models 1-3), as well as model 4 which has 1000 m thick ice on the shelf until 21 ka followed by restricted island-only ice, do not predict a Holocene highstand (Figure 8). The modelled RSL curves are dominated by the global GIA signal with the highest modelled sea level occurring at the present day. The field data provides strong evidence for a period of post-LGM sea level higher than present, which suggests that the restricted ice models do not contain enough local mass to result in a solid earth deformation to fit the geomorphological data, even with the extreme 3000 m thick ice in model 3.

The extensive shelf-edge model with only 100 m of ice (model 5) also does not predict RSL above present (Figure 8). It is only in the load scenarios where the ice thickness is increased to 1000 m in extensive models 6-8 do the outputs predict a period of RSL above present (Figure 8 and S6), demonstrating the importance of local GIA overprinting the far-field derived RSL. In model 6 (18 ka deglaciation) a 0.8 m highstand occurs at 5 ka, and in model 7 (15 ka deglaciation) a 4.2 m highstand occurs at 9 ka. Model 8 (12 ka deglaciation) has a double peaked highstand of 15.9 m at 13 ka, followed by a second of 13.0 m at 9 ka. This is the only model which predicts sea level far above the ca. 6-10 m marine limit implied by the geomorphological sea-level data (Figure 3). The timing of deglaciation in model 8 is also much too late to fit with the evidence of the onset of ice-free conditions at Tønsberg Point (Rosqvist et al., 1999). The output provides a useful maximum load end-member, but we are able to reject this solution. The extensive thick shelf-edge ice loads in models 6 and 7 provide the closest fit with the geomorphological sea-level data, with the higher highstand in model 7 of ca. 4 m, nearest in elevation to the measured marine limit, suggesting this is the optimum scenario. Crucially we find that an extensive thick model with relatively early deglaciation can simulate a highstand of similar timing and magnitude as the field data.

To test the sensitivity of the results with respect to changes in the rheology of the Earth, we combine the deglaciation model 7 with different viscosity profiles (Figure 9), keeping fixed the lithospheric thickness at the ICE-5G(VM2) value of 90 km since we know that this parameter plays a minor role in the GIA response (see Stocchi and Spada, 2009). It should be noted that the results in Figure 9 have mainly a qualitative character, since modifying the VM2 viscosity profile alters the agreement of the ICE-5G (VM2) predictions with the set of global Holocene RSL curves used to calibrate it. As pointed out by Tamisiea (2011), more realistic GIA estimates could be obtained by simultaneously varying the global ice loading history and the rheology, and possibly taking 3D variations in the Earth's properties into account, which is beyond the scope of this work. Due to the relatively small

sensitivity of the RSL curves to the site location (Figure 8), we only consider the site of Brown Mountain GPS (Table 3) in Figure 9. The ranges for the local upper mantle viscosity and the lower mantle viscosity are 0.2 to 0.8 x 10^{21} Pa s and 1.0 to 5.0 x 10^{21} Pa s, respectively. It is apparent that when the ICE-5G(VM2) upper mantle viscosity is used (0.5 x 10^{21} Pa s), a satisfactory fit with the data is obtained for all the lower mantle viscosities considered (the insensitivity to lower mantle viscosity is explained by the relatively small size of the ice load). The misfit increases when the upper mantle viscosity is too low (0.2 x 10^{21} Pa s, which implies a fast relaxation) or too high (0.8 x 10^{21} Pa s, which enhances the amplitude of the highstand) compared to the VM2 value.

Discussion

Testing models of LGM ice extent on South Georgia

The results of the GIA modelling presented in this paper, when compared to marine limit and RSL data, support the extensive glaciation hypothesis where LGM ice extends to the continental shelf edge (Clapperton et al., 1989; Graham et al., 2008; Sugden and Clapperton, 1977). Even with an extreme ice thickness of 3000 m (which is higher than the elevation of the highest summit, Mount Paget, and does not allow for underlying topography) in the restricted island-only model 3, the GIA outputs cannot produce a highstand to produce a ca. 6-10 m marine limit. Therefore, based upon GIA modelling, it seems unlikely that the restricted glaciation model of Bentley et al. (2007) is valid. The model (7) which provides the best fit with the data, suggests deglaciation of the shelf at ca. 15 ka BP. This is potentially ca. 4 ka later than suggested by the onset of lake sedimentation at Tønsberg Point (Rosqvist et al., 1999). A limitation of our approach is the lack of a spatially variable load and accounting for the underlying topography. It remains possible to fit the RSL data with an extensive ice cap model together with a spatially and temporally variable deglacial history to accommodate early deglaciation at Tønsberg, but this is beyond the scope of this study. This could be revisited when evidence for early deglaciation is found in more than one location.

356 The results of an extensive LGM ice cap on South Georgia requires the reinterpretation of existing
357 research. As proposed by Graham et al. (2008) this implies that terrestrial and fjord moraines
358 mapped by Bentley et al. (2007) and Hodgson et al. (2014a) are in fact either retreat, stillstand or
359 readvance margins of a post-LGM ice cap, formed subsequently to the maximum extension of the ice
360 onto the continental shelf. The moraines mapped by Graham et al. (2008) at the shelf edge are
361 therefore most likely to be LGM in age and a programme of offshore dating could establish this.
362 Both Sugden and Clapperton (1977) and Hodgson et al. (2014a) suggest that the offshore evidence
363 of glacial erosion may be from a previous Pleistocene extensive glaciation. However, we are able to
364 produce modelled elevations of RSL which fit with the geomorphological data based upon the
365 simplest explanation of a large LGM ice cap, avoiding the complication of multiple phases of GIA
366 through multiple glacial-interglacial cycles.
367
368 Our results also have implications for the long-term evolution of the island. Given the difficulty of
369 producing substantive highstands in the GIA models, even with a very substantial extensive ice cap it
370 seems unlikely that the rock platforms could have been formed at their current elevations (20-50m)
371 due to GIA alone. This is particularly apparent when their size is taken into account as they would
372 potentially have needed substantial periods of time to be eroded. It seems more likely that they may
373 have formed during one or more previous interglacial highstands, implying long-term uplift of the
374 island. We also cannot rule out that the platforms are entirely pre-glacial. Long-term uplift is
375 consistent with thermochronological data that suggest the island may have seen significant
376 exhumation since 10 Ma (Carter et al., 2014). Given that the platforms have survived at least one
377 glaciation, possibly several, we suggest that the LGM ice cap on South Georgia was not particularly
378 efficient at eroding pre-existing deposits (e.g. preserved beach material up to 52 m asl) or the higher
379 rock platforms. The non-erosion of more extensive raised beaches and enclosed marine fauna on
380 Prince Karls Forland on western Svalbard (Evans and Rea, 2005; Landvik et al., 2005; Mangerud et al.,
381 1996; Miller et al., 1989) and on eastern Baffin Island (Davis et al., 2006), even though they have

been overrun by glacier ice, constitute examples of similarly ineffective glacial erosion of pre-existing deposits at low elevations around the margins of an ice sheet-covered archipelago similar to South Georgia. Whether, like the Svalbard and Baffin Island examples, the survival of raised marine features was related to cold-based ice sheet marginal conditions or just localized ineffective erosion cannot be determined at this stage.

Ongoing land-level change on South Georgia

The available RSL data that constrains our GIA models is limited and precludes the development of a spatially variable ice load model. Aside from collecting further geomorphological evidence of RSL change, there may be potential to further constrain the spatial and temporal ice history of future models using instrumental data based upon the spatial pattern of modern rates of land-level change. The first global navigation satellite system (GNSS) station in South Georgia was installed on Brown Mountain (station: KEPA), King Edward Point in February 2013 with the aim of providing a reference point for the King Edward Point tide gauge and constrain tectonic motion of South Georgia (Teferle, *pers. comm*.). Three additional stations were installed in October 2014 at northern (SOG2), southern (SOG1) and eastern (SOG3) locations in South Georgia (Dalziel, *pers. comm.*). The short duration of the records means they are not yet suitable to use as constraints in this study, but a network of GPS locations providing detailed information as to the spatial pattern of present day rates of land-level change may help resolve model outputs further and allow for more complex ice load histories to be tested in the absence of geomorphological constraints. In the meantime, using the ALMA outputs of the local ice cap in Model 7 (Figure 8) and outputs from SELEN (Figure 6), we are able to provide estimates of present rates of vertical uplift at the four GPS sites as explained by the local and global modelled GIA (Table 3). Differences between these estimates and measured vertical rates may be ascribable to tectonics, local GIA or the selected Earth model (Figure 9).

Model observer	**Nearest**	**Local ice history**	**Global ice history**	**Total modelled**

location Longitude and Latitude (deg)	GNSS station	(ALMA) modelled uplift (mm yr^{-1})	(SELEN) modelled uplift (mm yr^{-1})	GIA uplift (mm yr^{-1})
Brown Mountain -36.50 -54.30	KEPA	0.52	0.45	0.97
Annenkov Island -37.04 -54.49	SOG3	0.44	0.44	0.88
Northwest South Georgia -38.05 -54.00	SOG2	0.37	0.46	0.83
Southeast South Georgia -36.04 -54.87	SOG1	0.43	0.42	0.85

Table 3 – Modelled rate of vertical displacement due to post-LGM glacial isostatic adjustment as computed by the models detailed in this paper at the four GPS locations on South Georgia. Locations from N. Teferle, (*pers. comm*.) and Dalziel, (*pers. comm*.). More information is available at https://www.unavco.org/data/gps-gnss/gps-gnss.html

Wider implications of an extensive LGM ice cap on South Georgia

The suggestion of an extensive thick ice cap on South Georgia has implications for other sub-Antarctic islands, on which limited geomorphological evidence is recorded, but where there exists similar debate about the extent of Quaternary glaciation(s) (Hodgson et al., 2014b; Sugden and Clapperton, 1977). If a large LGM ice cap existed in South Georgia then there is potential for the same to have occurred on other sub-Antarctic islands within a similar climatic context e.g. Kerguelen, and also fits with other models of extensive LGM ice proposed for Heard, Bouvet and the South Orkney Islands (Hodgson et al., 2014b). The presence of an extensive LGM ice cap that reached the continental shelf edge around South Georgia suggests affinity with West Antarctica and the Antarctica Peninsula, which also experienced the most extensive glaciation at the LGM, rather than with Patagonia where the greatest glacial extents were earlier in the Quaternary (Darvill et al., 2015). Our model results suggests that deglaciation on South Georgia occurred ca. 15 ka, which fits with geomorphological data from the east Antarctic Peninsula where initial retreat was underway by ~18-17.5 ka (Bentley et al., 2014), as well as dates of the onset of peat formation and lake

sedimentation at other sub-Antarctic islands, including Kerguelen, Auckland and Campbell, around this time (Hodgson et al., 2014b).

Our conclusion of an extensive ice cap extending to the shelf edge would imply that if there were any biological refugia around South Georgia, they must have been relatively localised and restricted to the outermost shelf and any potential nunataks. Our model is not spatially variable and so we are unable to determine the locations of these refugia using current datasets. Our fits with a recent assessment of the seabed biodiversity around South Georgia which concludes that most of the shelf is still undergoing recolonization following glacial retreat (Barnes et al., 2016).

The approach presented here, to use GIA modelling and associated RSL data to differentiate between opposing models of ice extent, may also be applied in other locations where similar debates exist, e.g. Iceland (Brader, 2015). The order-of-magnitude difference of the modelled RSL changes as a result of the maximum versus minimum ice extent models, means this approach is able to provide a first order test of the hypotheses without the need for detailed glacial histories. This is particularly valuable where offshore data is limited or lacks a chronology. However, not all current GIA models are designed to work at the sufficiently high enough number of spherical harmonics required to resolve differences between relatively small ice loads. Thus, a bespoke solution, such as used here with the flexible code in SELEN and ALMA (Spada, 2008; Spada et al., 2012; Spada and Stocchi, 2007), may be required.

Conclusions

We conclude from our GIA modelling and constrained by a newly-compiled RSL dataset, that the LGM glaciation of South Georgia was extensive and extended to the shelf edge at a time when the island was covered by thick (>1000 m) ice. Deglaciation occurred relatively early, indeed our best fit model suggests substantial deglaciation by ca. 15 ka BP, although independent data suggests this

may have been as early as 18 ka in places. Further work should seek to define the geometry of the South Georgia ice cap and the date and timing of deglaciation in order to allow the development of a more sophisticated and spatially-variable ice model. This will also require the collection of additional sea level index points to constrain the modelled outputs, and comparison of GPS-derived uplift rates to our GIA modelled present day rates of change.

Acknowledgements

We thank the Royal Scottish Geographical Society (RSGS), Carnegie Trust for the Universities of Scotland, and National Geographic for fieldwork support and to the members of the RSGS *Scotia* expedition for field assistance. We are also grateful to the Government of South Georgia and the South Sandwich Islands for permits and assistance in our work. This paper has benefited from discussions with Alastair Graham (who also provided Figure 1A), Dominic Hodgson and Pippa Whitehouse, members of PALSEA2 (an INQUA International Focus Group and a PAGES working group) and the Quaternary Research Association Sea Level and Coastal Change (SLaCC) working group. G.S. is funded by Programma Nazionale di Ricerche in Antartide (PNRA) 2013/B2.06 (CUP D32I14000230005). Reviewers by Alex Simms and an anonymous reviewer improved this manuscript.

List of Figures

Figure 1: Location Maps of South Georgia. (a) Summary map of bathymetry and geomorphology of South Georgia and its surrounding continental shelf (from Graham et al., 2008). Fault (dot-dash line) inferred from onshore expression of strike-strike fault (solid line) in the south east of the island. TMF, trough mouth fan. (b) Location Map of South Georgia. All place names are taken from map: South Georgia 1:200k, British Antarctic Survey Misc Sheet 12A and 12B. Red crosses mark locations of model predictions, including GPS sites in Table 3). (c) Raised beaches around South Georgia. Dots are scaled according to size and the elevation (m asl) of the *highest* beach or marine limit is shown beside symbol. (d) Rock platforms around South Georgia. Dots are scaled according to size and the elevation (m asl) of the rock platform is shown beside symbol.

Figure 2: Photographs of examples of the coastal geomorphology of South Georgia. A) Upper (7 m asl) and lower (3 m asl) shorelines at Antarctic Bay, B) Raised beaches at the snout of the Nordensjold in Cumberland Bay, C) Raised beaches at Moraine Fjord, and D) Raised beaches at Sandebugten, Barff Peninsula. E) Rock platforms at Stromness Bay, F) Rock platform at Tønsberg Peninsula, G) Rock platforms at Carlita Bay and H) Rock platform at Tønsberg Peninsula.

Figure 3: Relative sea-level data for South Georgia (from Table 1). Blue band gives 6-10 m typical range of highest raised beaches mapped on the island (references in text and supplementary information Tables S1 and S2). Dotted line joins the maximum and minimum ages of the formation of the raised beach at St Andrews Bay.

Figure 4: Topographic and geologic cross section through the centre of Enten Valley from Cumberland Fjord (left) ~400 m west to a small beach-dammed lake (right). Luminescence ages are

494 shown with field/lab codes (detailed in Table S3), while major beach ridges are labelled E1-7, though
495 E5 is not well expressed on this transect and not marked.
496
497 **Figure 5:** Sulphur counts (black line 2mm and grey line 2cm running average) obtained with an XRF
498 core scanner for core Co1305 (1042 to 978 cm depth) from Little Jason Lagoon. Line scan image of
499 the core section containing the lacustrine/marine transition. Grey bar indicates the position of
500 increase in sulphur. Arrow indicates position of the radiocarbon dated plant remains.
501
502 **Figure 6:** A: Map of present day rates of relative sea-level change modelled in SELEN using ICE-5G
503 and a VM2 average viscosity (details on Figure). B: Relative sea-level changes due to global GIA at
504 South Georgia (dotted line) are similar to the global (eustatic) changes in ice volume in ICE-5G (solid
505 line).
506
507 **Figure 7:** Disc ice loads extents in ALMA for the extensive shelf (maximum) and restricted (minimum)
508 island-only models in Table 2. Colours match those in the ice thickness histories in Figure 8.
509
510 **Figure 8:** Modelled relative sea-level changes using the 8 ice models detailed in Table 2 plotted
511 against data from Figure 3 (note blue band of marine limit in Figure 3 shown as dotted line here for
512 simplicity). Relative sea-level curves are a combination of the ALMA modelled outputs in response
513 to the ice thickness changes plotted in each graph (colours correspond to the ice models in Figure 7)
514 combined with the South Georgia SELEN global model relative sea level in Figure 6B. Note, output
515 for all the 12 observer locations are plotted in a single colour as they are so similar it is not possible
516 to visually separate them.
517
518 **Figure 9:** Modelled relative sea-level changes at the Brown Mountain GPS station using ice model 7
519 (detailed in Table 2) and a range of upper and lower mantle viscosities (x 10^{21} Pa s) plotted against

520 relative sea level data from Figure 3. Earth model used in outputs in Figure 8 shown by grey dotted

521 line.

References

Adie, R.J., 1964. Sea level changes in the Scotia Arc and Graham Land, in: Adie, R.J. (Ed.), Antarctic Geology. North-Holland Publishing Company, Amsterdam, pp. 27-32.

Argus, D.F., Peltier, W.R., Drummond, R., Moore, A.W., 2014. The Antarctica component of postglacial rebound model ICE-6G_C (VM5a) based on GPS positioning, exposure age dating of ice thicknesses, and relative sea level histories. Geophysical Journal International 198, 537-563.

Barnes, D.K.A., Hodgson, D.A., Convey, P., Allen, C.S., Clarke, A., 2006. Incursion and excursion of Antarctic biota: past, present and future. Global Ecology and Biogeography 15, 121-142.

Barnes, D.K.A., Sands, C.J., Hogg, O.T., Robinson, B.J.O., Downey, R.V., Smith, J.A., 2016. Biodiversity signature of the Last Glacial Maximum at South Georgia, Southern Ocean. Journal of Biogeography, n/a-n/a.

Bentley, M.J., Evans, D.J.A., Fogwill, C.J., Hansom, J.D., Sugden, D.E., Kubik, P.W., 2007. Glacial geomorphology and chronology of deglaciation, South Georgia, sub-Antarctic. Quaternary Science Reviews 26, 644-677.

Bentley, M.J., Ó Cofaigh, C., Anderson, J.B., Conway, H., Davies, B., Graham, A.G.C., Hillenbrand, C.-D., Hodgson, D.A., Jamieson, S.S.R., Larter, R.D., Mackintosh, A., Smith, J.A., Verleyen, E., Ackert, R.P., Bart, P.J., Berg, S., Brunstein, D., Canals, M., Colhoun, E.A., Crosta, X., Dickens, W.A., Domack, E., Dowdeswell, J.A., Dunbar, R., Ehrmann, W., Evans, J., Favier, V., Fink, D., Fogwill, C.J., Glasser, N.F., Gohl, K., Golledge, N.R., Goodwin, I., Gore, D.B., Greenwood, S.L., Hall, B.L., Hall, K., Hedding, D.W., Hein, A.S., Hocking, E.P., Jakobsson, M., Johnson, J.S., Jomelli, V., Jones, R.S., Klages, J.P., Kristoffersen, Y., Kuhn, G., Leventer, A., Licht, K., Lilly, K., Lindow, J., Livingstone, S.J., Massé, G., McGlone, M.S., McKay, R.M., Melles, M., Miura, H., Mulvaney, R., Nel, W., Nitsche, F.O., O'Brien, P.E., Post, A.L., Roberts, S.J., Saunders, K.M., Selkirk, P.M., Simms, A.R., Spiegel, C., Stolldorf, T.D., Sugden, D.E., van der Putten, N., van Ommen, T., Verfaillie, D., Vyverman, W., Wagner, B., White, D.A., Witus, A.E., Zwartz, D., 2014. A community-based geological reconstruction of Antarctic Ice Sheet deglaciation since the Last Glacial Maximum. Quaternary Science Reviews 100, 1-9.

Bevis, M., Melini, D., Spada, G., 2016. On computing the geoelastic response to a disk load. Geophysical Journal International 205, 1804-1812.

Brader, M.D., 2015. Postglacial relative sea-level changes and the deglaciation of northwest Iceland, Department of Geography. Durham University.

Carter, A., Curtis, M., Schwanethal, J., 2014. Cenozoic tectonic history of the South Georgia microcontinent and potential as a barrier to Pacific-Atlantic through flow. Geology 42, 299-302.

Clapperton, C.M., 1971. Geomorphology of the Stromness Bay-Cumberland Bay area, South Georgia, British Antarctic Survey Scientific reports No. 70. Natural Environment Research Council.

Clapperton, C.M., Sugden, D.E., Birnie, J., Wilson, M.J., 1989. Late-glacial and Holocene glacier fluctuations and environmental change on South Georgia, Southern Ocean. Quaternary Research 31, 210-228.

Clapperton, C.M., Sugden, D.E., Birnie, R.V., Hansom, J.D., Thom, G., 1978. Glacier fluctuations in South Georgia and comparison with other island groups in the Scotia Sea, in: Bakker, V.Z. (Ed.), Antarctic Glacial History and World Palaeoenvironments, Balkema Rotterdam.

Cook, A.J., Poncet, S., Cooper, A.P.R., Herbert, D.J., Christie, D., 2010. Glacier retreat on South Georgia and implications for the spread of rats. Antarctic Science 22, 255-263.

Darvill, C.M., Bentley, M.J., Stokes, C.R., Hein, A.S., Rodés, Á., 2015. Extensive MIS 3 glaciation in southernmost Patagonia revealed by cosmogenic nuclide dating of outwash sediments. Earth and Planetary Science Letters 429, 157-169.

Davis, P.T., Briner, J.P., Coulthard, R.D., Finkel, R.W., Miller, G.H., 2006. Preservation of Arctic landscapes overridden by cold-based ice sheets. Quaternary Research 65, 156-163.

Evans, D.J.A., Rea, B.R., 2005. Late Weichselian deglaciation and sea level history of St Jonsfjorden, Spitsbergen: A contribution to ice sheet reconstruction. Scottish Geographical Journal 121, 175-201.

Gordon, J.E., Hansom, J.D., 1986. Beach Forms and Changes Associated with Retreating Glacier Ice, South Georgia. Geografiska Annaler. Series A, Physical Geography 68, 15-24.

573 Gordon, J.E., Haynes, V.M., Hubbard, A., 2008. Recent glacier changes and climate trends on South
574 Georgia. Global and Planetary Change 60, 72-84.
575 Gordon, J.E., Timmis, R.J., 1992. Glacier fluctuations on South Georgia during the 1970s and early
576 1980s. Antarctic Science 4, 215-226.
577 Graham, A.G.C., Fretwell, P.T., Larter, R.D., Hodgson, D.A., Wilson, C.K., Tate, A.J., Morris, P., 2008. A
578 new bathymetric compilation highlighting extensive paleo–ice sheet drainage on the continental
579 shelf, South Georgia, sub-Antarctica. Geochemistry, Geophysics, Geosystems 9, n/a-n/a.
580 Gregory, J.W., 1915. The physiography of South Georgia as shown by Mr Ferguson's photographs, in:
581 Ferguson, D. (Ed.), Geological Observations in South Georgia, Transactions of the Royal Society of
582 Edinburgh, pp. 814-816.
583 Hall, B.L., 2009. Holocene glacial history of Antarctica and the sub-Antarctic islands. Quaternary
584 Science Reviews 28, 2213-2230.
585 Hansom, J.D., 1979. Beach Form and Process Variation in South Georgia, a sub-Antarctic Island.
586 University of Aberdeen, Unpublished PhD thesis.
587 Hodgson, D.A., Graham, A.G.C., Griffiths, H.J., Roberts, S.J., Cofaigh, C.Ó., Bentley, M.J., Evans, D.J.A.,
588 2014a. Glacial history of sub-Antarctic South Georgia based on the submarine geomorphology of its
589 fjords. Quaternary Science Reviews 89, 129-147.
590 Hodgson, D.A., Graham, A.G.C., Roberts, S.J., Bentley, M.J., Cofaigh, C.Ó., Verleyen, E., Vyverman,
591 W., Jomelli, V., Favier, V., Brunstein, D., Verfaillie, D., Colhoun, E.A., Saunders, K.M., Selkirk, P.M.,
592 Mackintosh, A., Hedding, D.W., Nel, W., Hall, K., McGlone, M.S., Van der Putten, N., Dickens, W.A.,
593 Smith, J.A., 2014b. Terrestrial and submarine evidence for the extent and timing of the Last Glacial
594 Maximum and the onset of deglaciation on the maritime-Antarctic and sub-Antarctic islands.
595 Quaternary Science Reviews 100, 137-158.
596 Hogg, A.G., Hua, Q., Blackwell, P.G., Niu, M., Buck, C.E., Guilderson, T.P., Heaton, T.J., Palmer, J.G.,
597 Reimer, P.J., Reimer, R.W., Turney, C.S.M., Zimmerman, S.R.H., 2013. SHCal13 Southern Hemisphere
598 Calibration, 0–50,000 Years cal BP.
599 Hogg, O.T., Barnes, D.K., Griffiths, H.J., 2011. Highly diverse, poorly studied and uniquely threatened
600 by climate change: an assessment of marine biodiversity on South Georgia's continental shelf. Plos
601 One 6, e19795.
602 Kelsey, H.M., 2015. Geomorphological indicators of past sea levels, Handbook of Sea-Level Research.
603 John Wiley & Sons, Ltd, pp. 66-82.
604 Landvik, J.Y., Ingolfsson, O., Mienert, J., Lehman, S.J., Solheim, A., Elverhoi, A., Ottesen, D., 2005.
605 Rethinking Late Weichselian ice-sheet dynamics in coastal NW Svalbard. Boreas 34, 7-24.
606 Mangerud, J., Jansen, E., Landvik, J.Y., 1996. Late Cenozoic history of the Scandinavian and Barents
607 Sea ice sheets. Global and Planetary Change 12, 11-26.
608 Miller, G.H., Sejrup, H.P., Lehman, S.J., Forman, S.L., 1989. Glacial history and marine environmental
609 change during the last interglacial-glacial cycle, western Spitsbergen, Svalbard. Boreas 18, 273-296.
610 Peltier, W.R., 2004. Global glacial isostasy and the surface of the ice-age earth: The ICE-5G (VM2)
611 model and GRACE. Annual Review of Earth and Planetary Sciences 32, 111-149.
612 Peltier, W.R., Argus, D.F., Drummond, R., 2015. Space geodesy constrains ice age terminal
613 deglaciation: The global ICE-6G_C (VM5a) model. Journal of Geophysical Research: Solid Earth 120,
614 450-487.
615 Purcell, A., Tregoning, P., Dehecq, A., 2016. An assessment of the ICE6G_C(VM5a) glacial isostatic
616 adjustment model. Journal of Geophysical Research: Solid Earth 121, 3939-3950.
617 Rosqvist, G.C., Rietti-Shati, M., Shemesh, A., 1999. Late glacial to middle Holocene climatic record of
618 lacustrine biogenic silica oxygen isotopes from a Southern Ocean island. Geology 27, 967-970.
619 Smith, J., 1960. Glacier problems in South Georgia. Journal of Glaciology 705-714.
620 Spada, G., 2008. ALMA, a Fortran program for computing the viscoelastic Love numbers of a
621 spherically symmetric planet. Computers & Geosciences 34, 667-687.
622 Spada, G., Melini, D., Galassi, G., Colleoni, F., 2012. Modeling sea level changes and geodetic
623 variations by glacial isostasy: the improved SELEN code. arXiv preprint arXiv:1212.5061.

624 Spada, G., Stocchi, P., 2007. SELEN: A Fortran 90 program for solving the “sea-level equation”.
625 Computers & Geosciences 33, 538-562.
626 Stocchi, P., Spada, G., 2009. Influence of glacial isostatic adjustment upon current sea level variations
627 in the Mediterranean. Tectonophysics 474, 56-68.
628 Stone, P., 1974. Physiography of the North-east coast of South Georgia, British Antarctic Survey
629 Bulletin, pp. 17-36.
630 Stone, P., 1976. Raised marine and glacial features of the Cooper Bay-Wirik Bay area, South Georgia,
631 British Antarctic Survey Bulletin. 44, 47-56.
632 Stone, P., 1979. Raised Marine features on the south side of Royal Bay, South Georgia, British
633 Antarctic Survey Bulletin, pp. 137-141.
634 Stuiver, M., Reimer, P.J., 1993. Extended 14C database and revised CALIB 3.0 radiocarbon calibration
635 program. Radiocarbon 35, 215-230.
636 Sugden, D.E., Clapperton, C.M., 1977. The maximum ice extent on island groups in the Scotia sea,
637 Antarctica. Quaternary Research 7, 268-282.
638 Sugden, D.T., John, B.S., 1973. The ages of glacier fluctuations in the South Shetland Islands,
639 Antarctica, Palaeoecology of Africa, the Surrounding Islands and Antarctica. Balkema, Cape Town,
640 pp. 141-159.
641 Tamisiea, M.E., 2011. Ongoing glacial isostatic contributions to observations of sea level change.
642 Geophysical Journal International 186, 1036-1044.
643 Thatje, S., Hillenbrand, C.-D., Mackensen, A., Larter, R., 2008. Life Hung by a Thread: Endurance of
644 Antarctic Fauna in Glacial Periods. Ecology 89, 682-692.
645 Tushingham, A.M., Peltier, W.R., 1991. Ice-3G: a new global model of late Pleistocene de-glaciation
646 based upon geophysical predictions of post-glacial relative sea level change. Journal of Geophysical
647 Research 96, 4497-4523.
648

Figure 1

Click here to download high resolution image

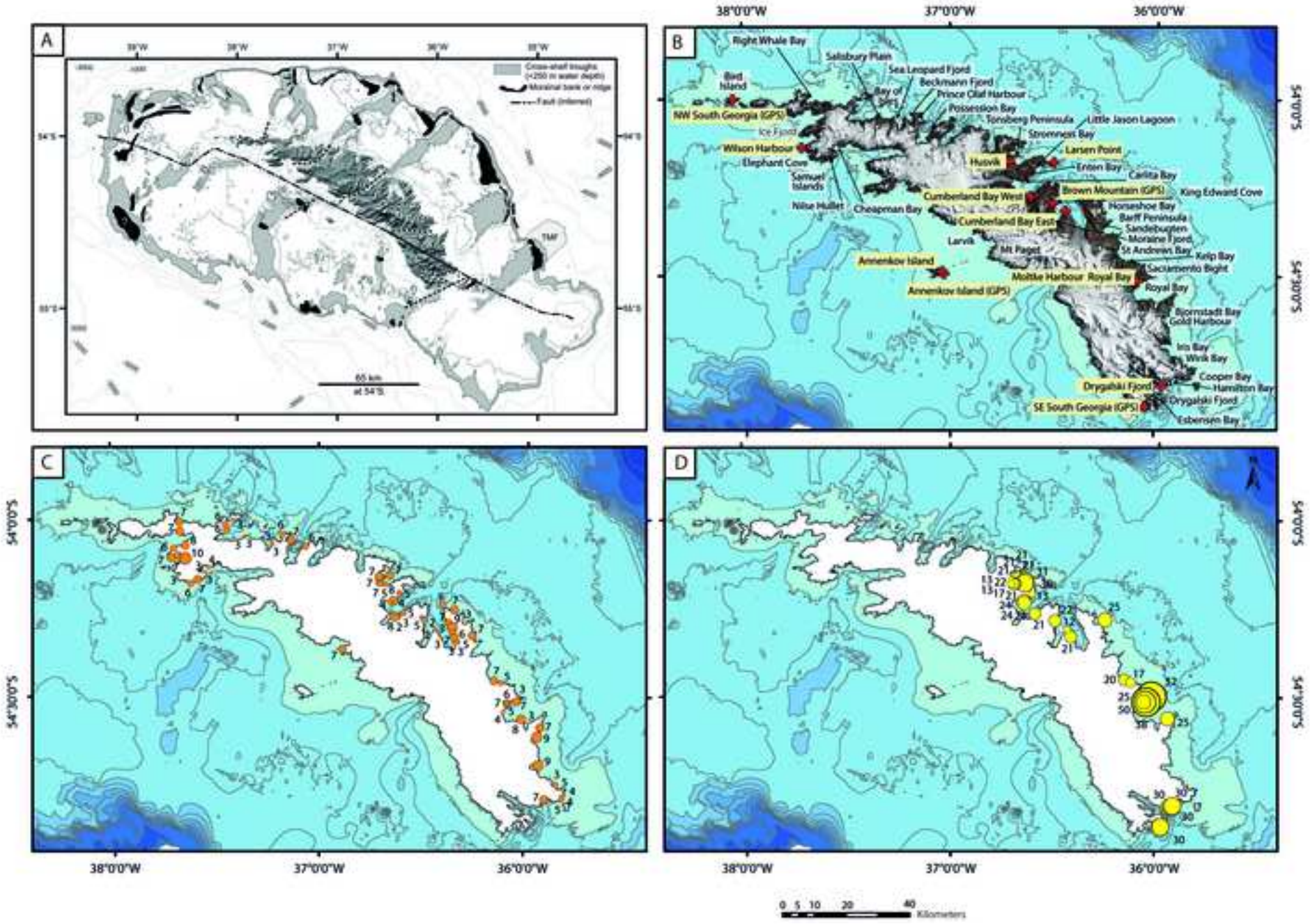

Figure 2

Click here to download high resolution image

Figure 3

Click here to download high resolution image

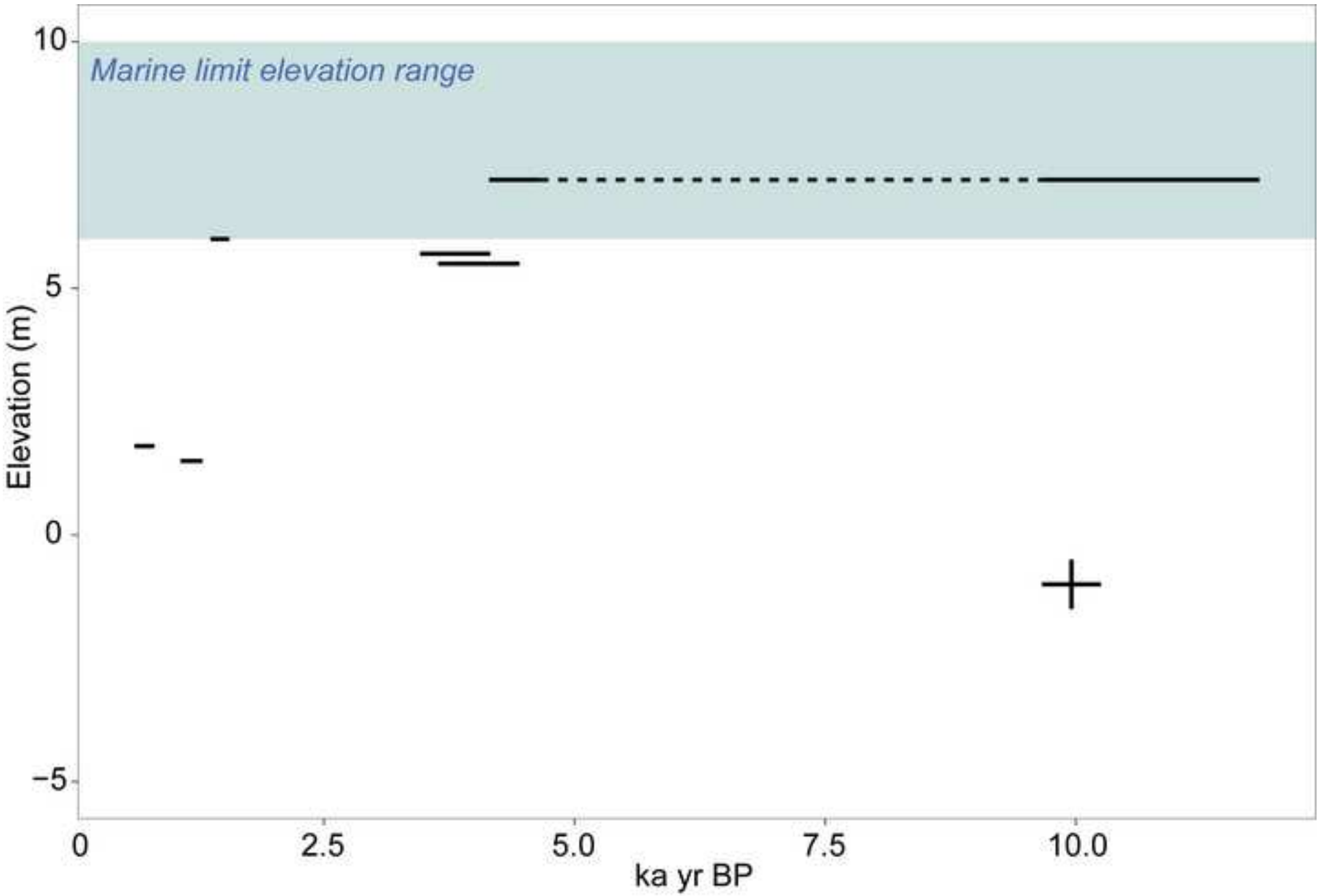

Figure 4

Click here to download high resolution image

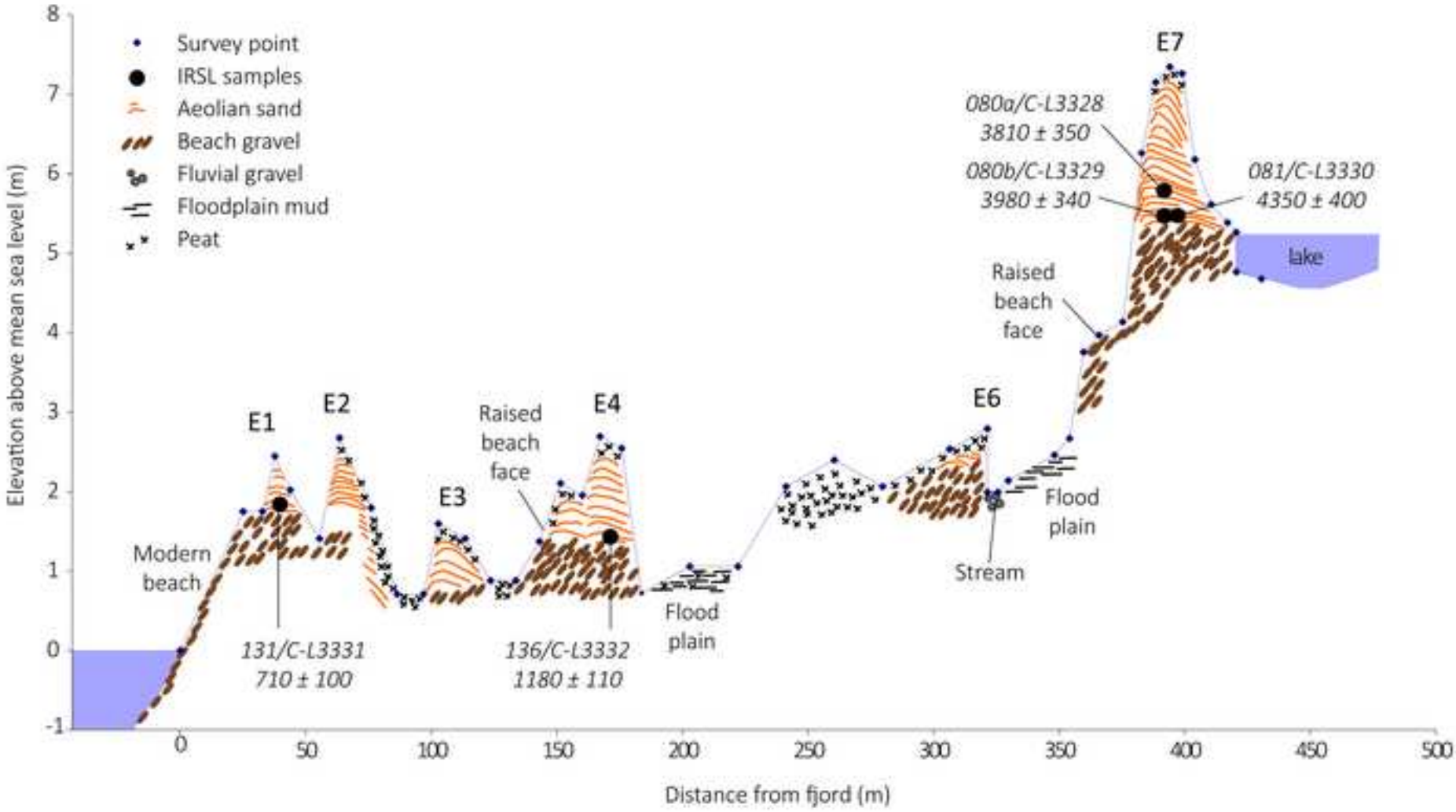

Figure 5

Click here to download high resolution image

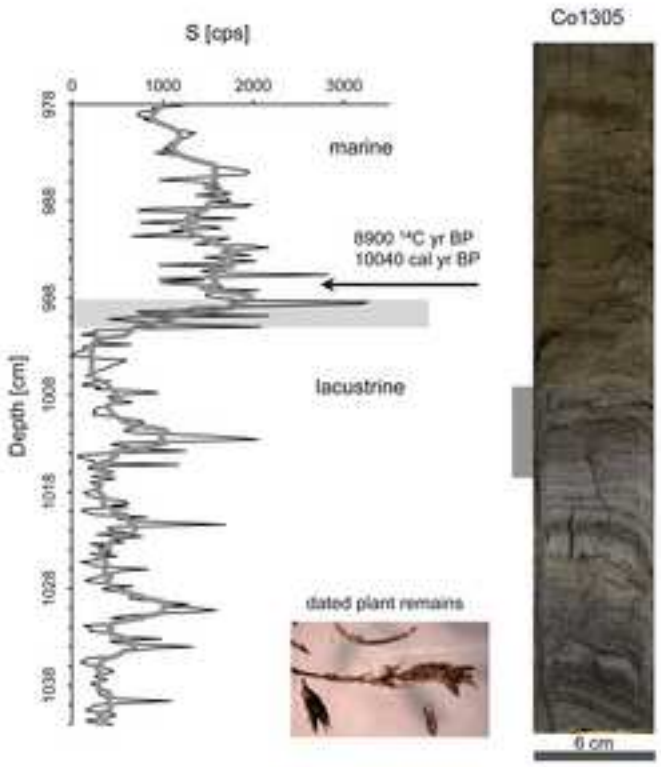

Figure 6

Click here to download high resolution image

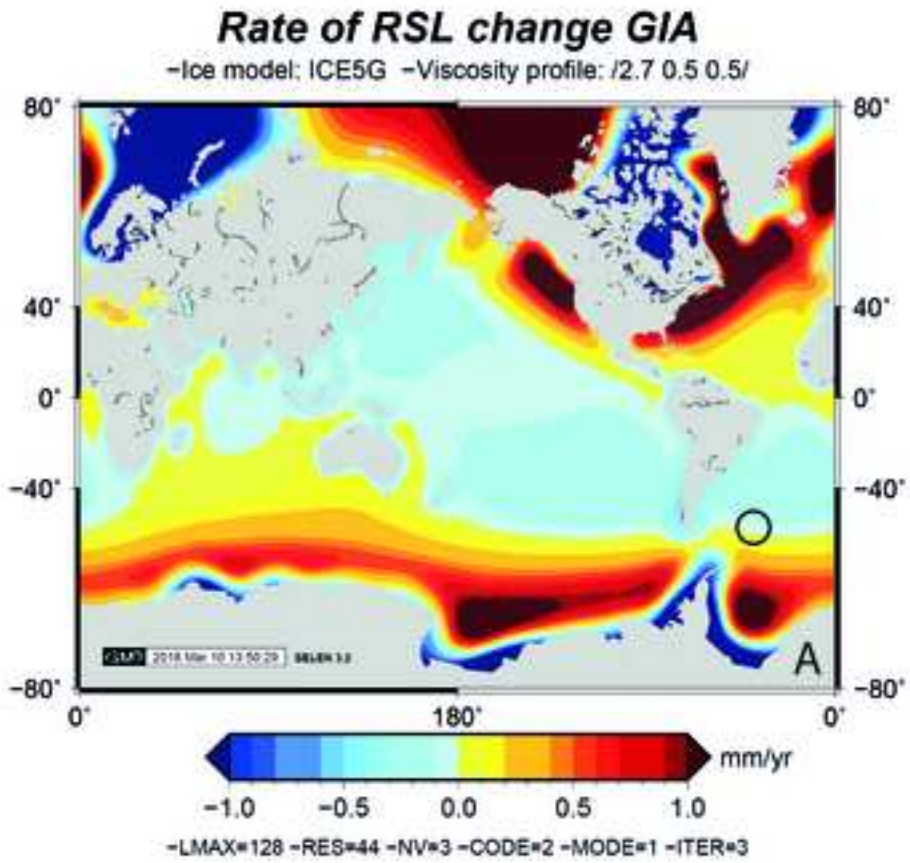

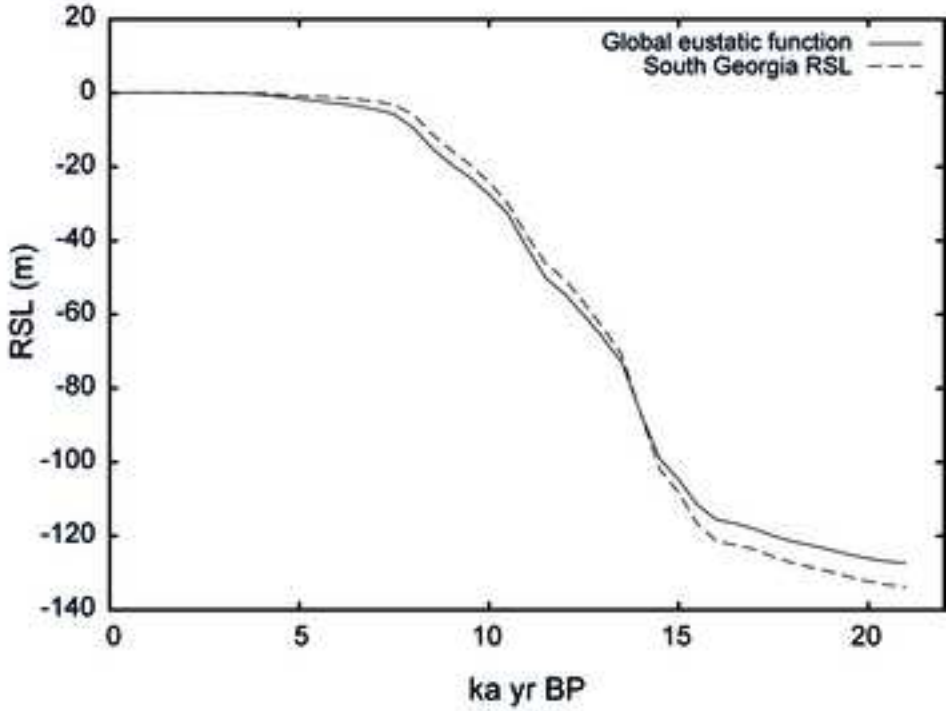

Figure 7

Click here to download high resolution image

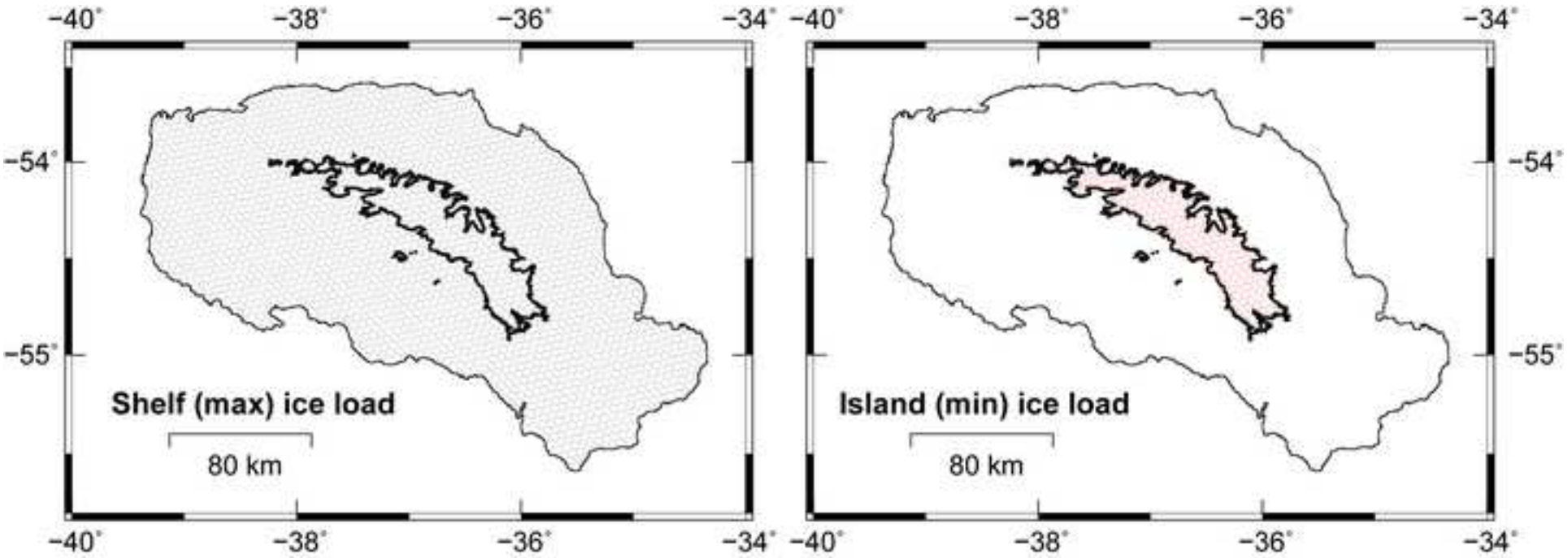

Figure 8

Click here to download high resolution image

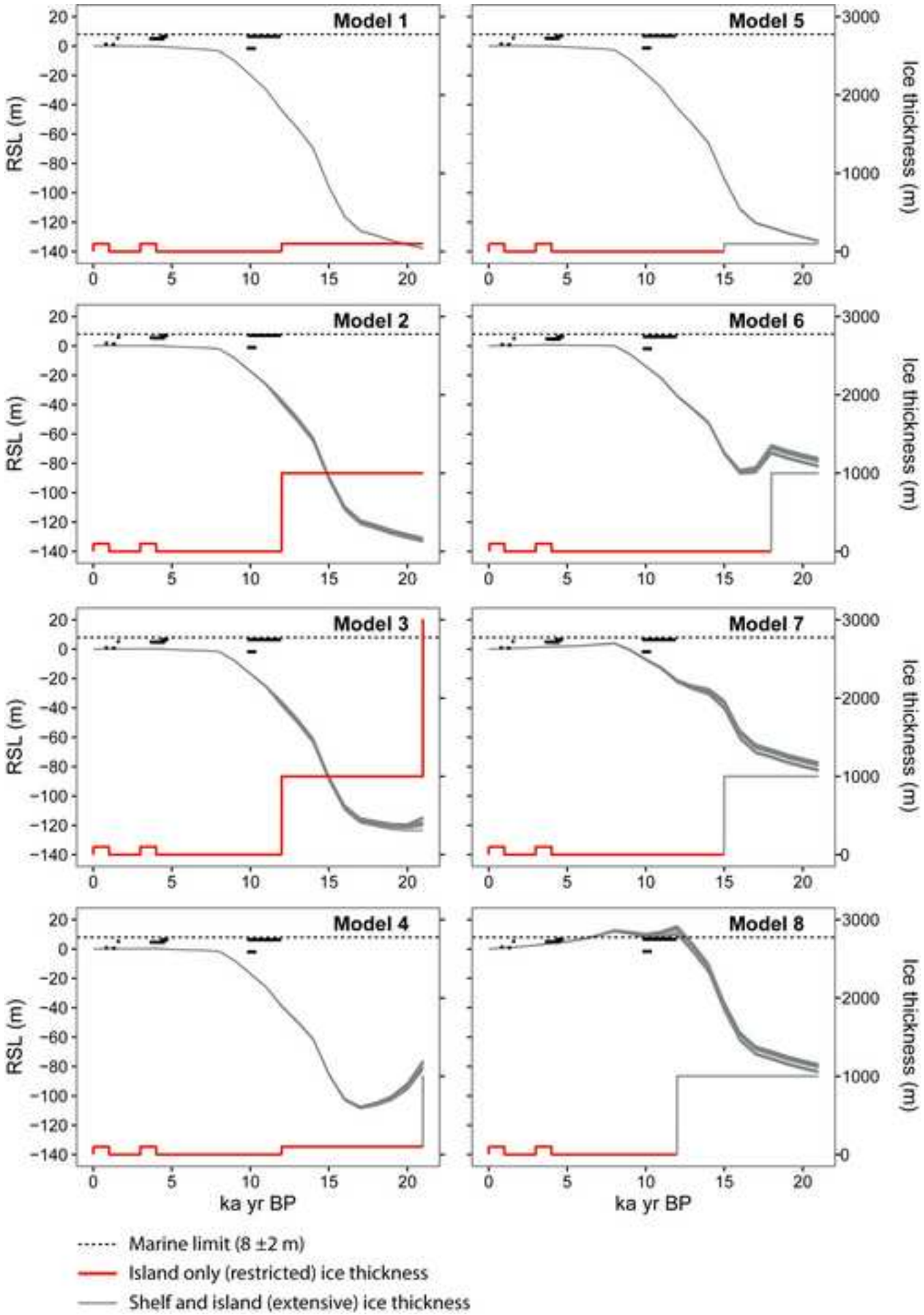

Figure 9

Click here to download high resolution image

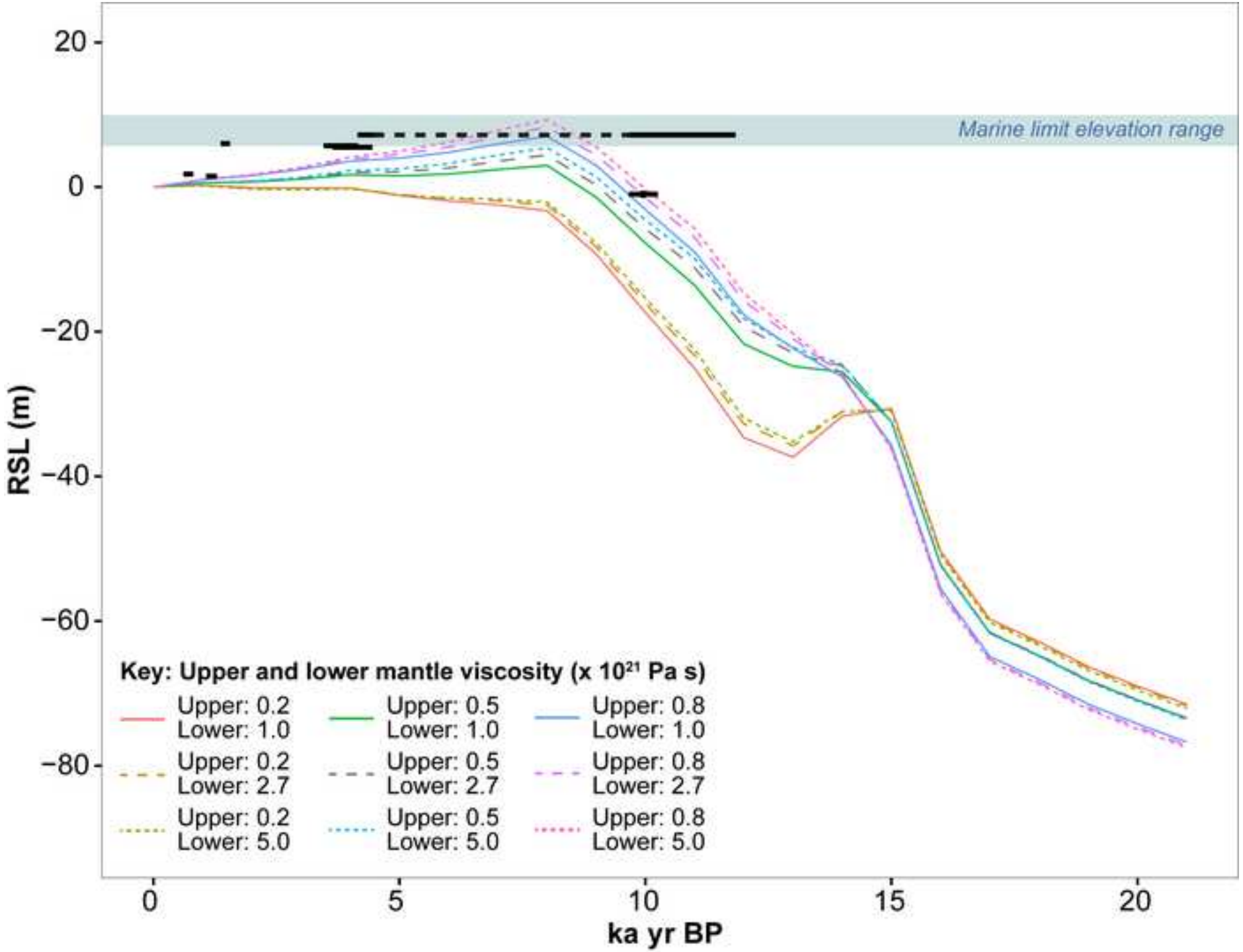

Supplementary Data

Click here to download Supplementary Data: Supp info - Barlow et al QSR South Georgia.pdf